Conformal Lattice Structure Design and Fabrication

Jason Nguyen[1], Sang-In Park[1], David W. Rosen[1], Luis Folgar[2], James Williams[2]

[1]School of Mechanical Engineering. Georgia Institute of Technology
[2]Paramount Industries, a 3D Systems Company

Abstract

One application of additive manufacturing is for fabrication of customized, light-weight material called Conformal Lattice Structures (CLS), a type of cellular structure with dimensions of 0.1 to 10 mm.   In this paper, two advances are reported for designing CLS.   First, computer-aided design technologies were developed for efficiently generating and representing CLS, given selected part model surfaces.   Second, a method is presented for efficiently optimizing CLS by utilizing a heuristic that reduces the multivariate optimization problem to a problem of only two variables. The heuristic is: stress distributions are similar in CLS and in a solid body of the same shape. Software will be presented that embodies this process and is integrated into a commercial CAD system.   In this paper, the method is applied to design strong, stiff, and light-weight Micro Air Vehicle (MAV) components.

1   Introduction

1.1   Additive Manufacturing

Additive manufacturing (AM) refers to the use of layer-based additive processes to manufacture finished parts by stacking layers of thin 2-D cross-sectional slices of materials. This process enable fabrication of parts with high geometric complexity, material grading, and customizability [1].

Design for manufacturing (DFM) has typically meant that designers should tailor their designs to eliminate manufacturing difficulties and minimize costs.   However, the improvement of AM technologies provides an opportunity to re-think DFM to take advantage of the unique capabilities of these technologies [2].   Several companies are now using AM technologies for production manufacturing.   For example, Siemens, Phonak, Widex, and the other hearing aid manufacturers use selective laser sintering (SLS) and stereolithography (SLA) machines to produce hearing aid shells, Align Technology uses SLA to fabricate molds for producing clear braces ("aligners"), and Boeing and its suppliers use SLS to produce ducts and similar parts for F-18 fighter jets.   In the first three cases, AM machines enable one-off, custom manufacturing of 10's to 100's of thousands of parts.   In the last case, AM technology enables low volume production. In addition, AM can greatly simplify product assembly by allowing parts that are typically manufactured as multiple components to be fabricated as one piece. More generally, the unique capabilities of AM technologies enable new opportunities for customization, improvements in product performance, multi-functionality, and lower overall manufacturing costs.   These unique capabilities include: shape complexity, where very complex shapes, lot sizes of one, customized geometries, and shape optimization are enabled; material complexity, where material can be processed one point, or one layer, at a time, enabling the manufacture of parts with complex material compositions and designed property gradients; and hierarchical

complexity, where multi-scale structures can be designed and fabricated from the microstructure through geometric mesostructure (sizes in the millimeter range) to the part-scale macrostructure.

In this paper, we cover two main topics. First, we present geometric construction methods that enable designers to take advantage of the shape complexity capabilities of AM processes. Specifically, we develop a method for constructing cellular materials that conform to the shapes of part surfaces; when restricted to lattice structures we call such constructs Conformal Lattice Structures[TM] (CLS). The software that embodies this process is integrated into a commercial computer-aided design (CAD) system. Second, we present a design method, the augmented size matching and scaling (SMS) method, to optimize CLS efficiently and systematically.

1.2 Cellular Materials

The concept of designed cellular materials is motivated by the desire to put material only where it is needed for a specific application. From a mechanical engineering viewpoint, a key advantage offered by cellular materials is high strength accompanied by a relatively low mass. These materials can provide good energy absorption characteristics and good thermal and acoustic insulation properties as well [3]. Cellular materials include foams, honeycombs, lattices, and similar constructions. When the characteristic lengths of the cells are in the range of 0.1 to 10 mm, we refer to these materials as mesostructured materials. Mesostructured materials that are not produced using stochastic processes (e.g. foaming) are called designed cellular materials. In this paper, we focus on designed lattice materials called meso-scale lattice structure (MSLS).

In the past 15 years, the area of lattice materials has received considerable research attention due to their inherent advantages over foams in providing light, stiff, and strong materials [4]. Lattice structures tend to have geometry variations in three dimensions; some of our designs are shown in Figure 1. Deshpande et al. point out that the strength of foams scales as $\rho^{1.5}$, whereas lattice structure strength scales as ρ, where ρ is the volumetric density of the material. As a result, lattices with a $\rho = 0.1$ are about 3 times stronger than a typical foam [5]. The strength differences lie in the nature of material deformation: the foam is governed by cell wall bending, while lattice elements stretch and compress.

In order to effectively design cellular structures, we must be able to accurately model, determine the mechanical properties, and quantify the performance of these structures. Many methods have been developed to analyze various cellular structures. For instance, Ashby et al. has conducted extensive research in the area of metal foams [4]. Wang and McDowell have performed a comprehensive review of analytical modeling, mechanics, and characteristics of various metal honeycombs [6, 7]. Deshpande et al. have investigated extensively lattice cells, particularly the octet-truss structure. However, the analysis assumed that the struts only experience axial forces [5], while Johnson et al. provided a more comprehensive analytical model of the truss structure by considering each
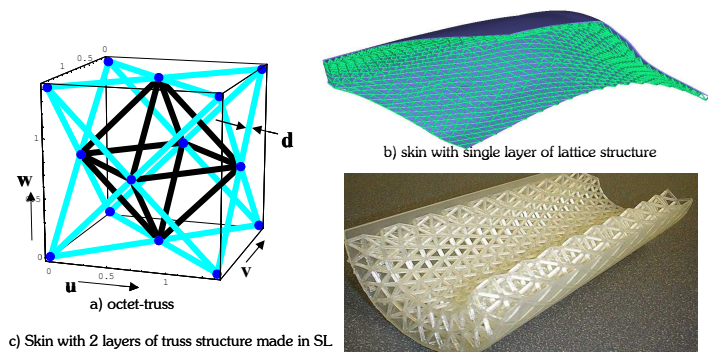

Figure 1: Octet truss unit cell and example parts with octet truss mesostructure.

strut as a beam experiencing axial, bending, shearing, and torsion effects. The octet-truss structure was analyzed using a unit-truss model that consists of a node and set of half-struts connecting to the node [8].

1.3 Design Methods

The design synthesis method for cellular materials consists of size, shape, and topology optimization to address different aspects of the structural design problem. In order to understand optimization of structures, the definitions of three categories of structural optimization are important [9]. A typical size optimization involves finding the optimal cross-sectional area of each strut in a truss structure [10]. Shape optimization computes the optimal form that defined by the boundary curves or boundary surfaces of the body [11, 12]. The process may involve moving nodes to change the shape of the structure; however, the element-node connectivity remains intact. Topology optimization, according to Rozvany, finds optimal connective or spatial sequences of members or elements in a structure [13]. In topological optimization, the physical size, shape, and connectivity of the structure are not known. The only known properties are the volume of the structure, the loads, and the boundary conditions [9]. It can be seen that topology optimization involves aspects of both size and shape optimization. Three categories of structural optimization are illustrated in Figure 2. It can be seen that size and shape optimizations consider the material distribution in the structure to satisfy certain loading conditions while maintaining the same topology. On the other hand, the initial and optimal structures are completely different in the case of topology optimization. In this research, optimization variables of the truss structures are strut diameters. However, each unit cell of the MSLS can have a different configuration depending on the selection criteria. Therefore, "topology optimization' will be the term used in this research for designing and optimizing MSLS.

Structural optimization for cellular structures dates as far back as a century ago. In 1904, George Michell, an Australian engineer, published a theory that defines the existence of an analytically optimal truss structure under certain loading conditions [14]. However, Michell trusses are limited to two dimensions and are not conducive to conventional manufacturing due to varying lengths and curved beams needed for optimal solution. Hence, it is very limited in application.
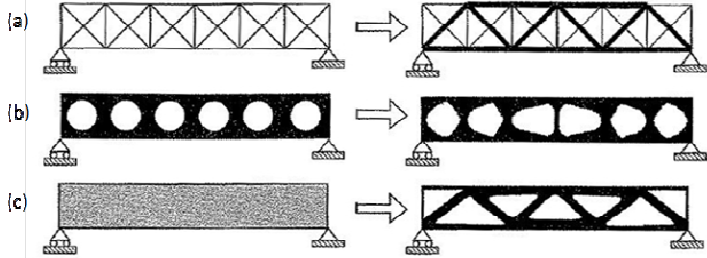

Figure 1: (a) Sizing optimization of a truss structure, (b) shape optimization, and (c) topology optimization [9]

The topology optimization techniques used to design truss structures are based on one of two approaches: the homogenization (continuum) approach and the ground (discrete) truss approach. The homogenization approach in topology optimization is a material distribution method that considers the design space as an artificial composite material with an infinite number of periodically distributed small holes. The problem is transformed from a topology optimization problem to a sizing optimization problem by considering the sizes of these small holes as design variables. The main task is to create a microstructure model using a material density function. In the final optimal structure, regions with density at or near one are filled

while regions with density at or near zero are empty. The method was pioneered by Bendsøe and Kikuchi in 1988 [15].

The ground truss approach starts with a ground structure, which is a grid of all elements connecting the nodes in the design space. The optimal truss structure is realized by selecting an optimal substructure from this pre-defined ground structure. Ultimately, the ground-truss approach is a sizing optimization problem, where the cross-sections of ground truss members are the continuous design variables for the optimization. The cross-sections of the struts are sized to support the applied loads on the structure. Struts with cross-sections near zero are then removed to obtain the optimal structure [16].

2   CLS Design Method

The basic idea of how cellular materials are created is presented here. Four example primitive cell types are shown in Figure 3, three of which are lattice structures and the fourth is a foam. These cell types are 2-dimensional for simplicity of presentation. The octet lattice in Figurea is an example 3-D cell type. Lattice structures consist of a set of struts (beams) that connect the nodes of the lattice.
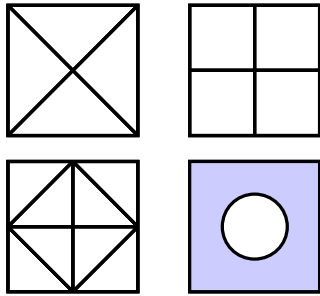
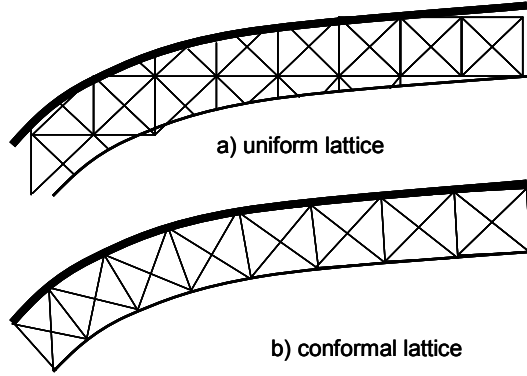Figure 3: Cellular primitives: three lattice structures and one web structure

a) uniform lattice

b) conformal lattice

Figure 4: Uniform and conformal lattice structures

To generate the cellular designs in Figure, the primitive cell types must be mapped into a mesh. In 2-D, the mesh consists of a set of connected quadrilaterals. In 3-D the mesh consists of hexahedra (6-sided volume elements with planar sides). The uniqueness of our work is our use of conformal cellular structures, rather than uniform "lattice block" materials, that can be used to stiffen or strengthen a complex, curved surface. To see the difference between conformal and uniform structures, Figure 4a is an example uniform lattice structure, while Figure 4b shows a conformal lattice. Meshes for uniform structures consist of cube elements in 3-D (squares in 2-D), while for conformal structures, the mesh elements are general hexahedra. We have developed a new algorithm for generating conformal meshes that are used to create conformal lattice and cellular structures. An older algorithm based on a mapped meshing approach [18] has been updated significantly. We prefer that mesh elements are as cubic as possible; i.e., are of uniform thickness and uniform size. Such meshes are typically not generated by the free meshing methods in finite-element analysis codes, while typical part geometries are too complex for mapped meshing methods.

2.1 CLS Construction Method

The overall method for generating conformal cellular structures is shown in Figure 5. It consists of two main steps, indicated by the shaded rectangles: computing 3D conformal mesh, and populating the mesh with cells. Inputs and outputs of the steps are shown as ovals. Each step is detailed below.

The objective of the meshing algorithm is to generate a conformal hexahedral mesh into which cells from the cell library can be placed. One or more layers of cellular structure can be placed to support the part's skin. The input to the algorithm may be a CAD solid model of the part, a surface model of the part, or a triangulated surface model (STL file) of the part. A method of constructing solid and STL models of lattice structures was presented in [17]. The method utilized the conformal lattice generation algorithm from [18].
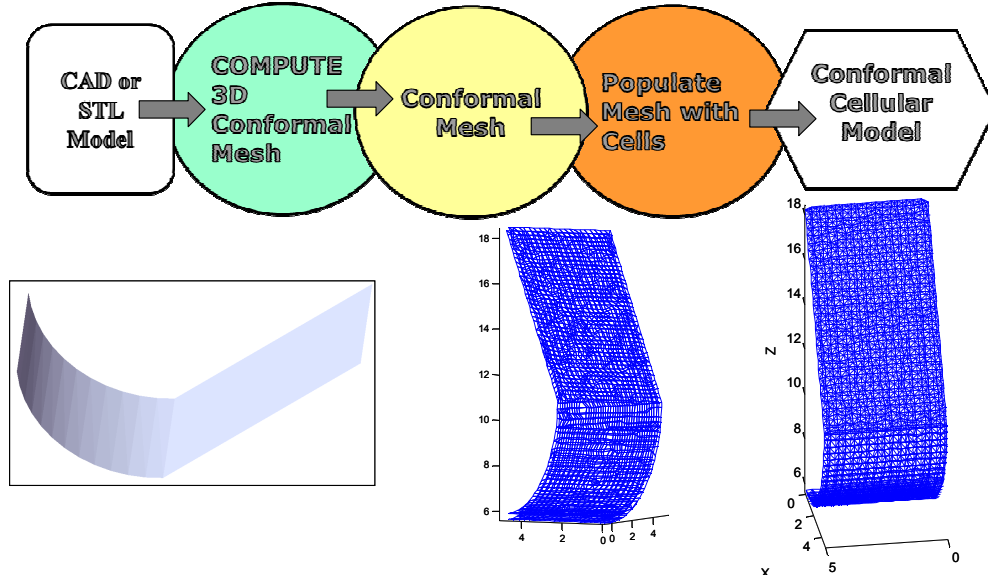

Figure 5: CLS construction method

2.2 Construct 3D Conformal Mesh

The algorithm to generate a 3-D conformal mesh is shown in Figure 6. The first step is to divide the part boundary into relatively flat regions, since it is easier to control the mesh generation method if regions are not very curved. We implement an absolute angular deviation measure between surface or triangle normal vectors to determine if that surface or triangle should be added to the region being generated. For the purposes of presentation, we will assume that a STL file was given. Then, one triangle is chosen as the first triangle of a region. The normal vector of each connected triangles is compared to the normal of the first triangle; if they differ by less than a given tolerance, the triangle is added to the region. As an example, the tolerance for the simple part in Figure 5 was chosen so that the model consists of two regions: the cylindrical surface and the planar surface.

For each region, three main steps are performed as indicated by lines 3, 4, 5 of Figure 6. The first is to compute the offset of the object boundary. An offset is a collection of points that are at a specified distance away from the starting surface (distance is called the offset distance). As

an example, an offset of a circle is a circle that is concentric with the first circle. Generally speaking, a positive offset results in a larger object, while a negative offset results in a smaller object. We use an offset method developed for tessellated part surfaces [19], but any offsetting method could be applied.

Algorithm Construct Conformal Mesh
Input: CAD or STL model, desired element size
Output: hexahedral mesh that conforms to the outer surface of the given model
1. Partition part model into relatively flat regions.
2. For each region,
3.   compute offset of region boundary
4.   construct tri-parameter volume
5.   divide parameterized volume into hexahedra
6. End for each region.
7. Ensure region boundaries match.

Figure 6: Algorithm for constructing a conformal mesh

The second step is to construct a tri-parameter volume between the original surface and its offset. Surfaces are parameterized using two parameters. Volumes are parameterized using three parameters. This step of the algorithm imposes a surface parameterization on the region of the part that will be reinforced [20]. The same parameterization is transferred to the offset surface. Finally, a lofted volume is constructed from the original surface to the offset surface.

The third step is to generate the conformal mesh by dividing the parameterized volume into individual elements (hexahedra). This is very straightforward. After selecting either the number of elements or their typical size, increments in each of the three parameters are computed, which are used to generate elements of the mesh. For example, if the increment in u is chosen to be 0.1, then 10 elements in the u direction will be generated, since $(1 - 0) / 0.1 = 10$. By successively incrementing each of the three parameters that define the tri-parametric volume, mesh elements are created.

The final step in Algorithm Construct Conformal Mesh (line 7) is to ensure that region boundaries match by adjusting node positions and by adding elements, if necessary. Since the regions are parameterized separately, the hexahedral elements may not match well. Nodes from neighboring regions may be moved and merged to achieve matched boundaries. Also, a series of hexahedral or tetrahedral elements may be added in gaps between meshes in neighboring regions.

2.3   Construct MSLS

The algorithm for the second step (populate mesh with cells) of the overall conformal cellular structure design method from Figure 6 is described here. One input to the algorithm is the conformal hexahedral mesh that was generated in the first step. The other input is the cell types contained within a library. The first step is to partition the mesh elements into regions such that within each region the loading conditions are similar on each element. These need not be the same regions that were used for mesh construction. For each region, a cell type from the cell type library is selected to populate the mesh elements in that region. The idea is to match the region's loading conditions to the cell type, such that the cell type is effective at supporting

the loading conditions. In this manner, the resulting cellular structure is more likely to be lighter for a given level of stress or deflection. These operations may be performed concurrently or maybe performed sequentially, depending upon the designer's preference and may be automated or be performed by the designer directly.

The final step in Figure 7, "Apply Selected Cell Types to Selected Mesh Elements," is where the actual cellular geometric model is constructed. This operation has been called population of mesh elements earlier. One simply maps a cell type into a mesh element. Since both the cell type and the mesh element are defined parametrically, a simple parametric mapping algorithm can be applied to directly construct cell geometry.

To construct a STL of the CLS, additional geometric construction operations must be performed. We utilize the approach described in [17], where solid models of the half-struts incident at each node of the mesh are constructed using Boolean operations in a solid modeling system. Then, each solid "node" is tessellated and the triangles are written to a STL file.

The resulting conformal cellular geometric model can be subjected to optimization methods in order to reduce weight, increase strength, increase stiffness, achieve some other objective, or achieve some combination of objectives. Such methods have been applied by a number of research groups [21].

2.4   Integration into CAD

The overall process for constructing MSLS has been embodied in a software package called TrussCreator, which is available as a plug-in for the Siemens NX CAD system. The construction procedure is shown in Figure 7. For each step, dialog boxes are designed and created for user input. The user can access these dialog boxes through the TrussCreator menu, as shown in Figure 8. In the lattice parameter setting menu, the user can input information about diameter of struts, the size of unit cells, and partition angle (step 1 in Figure 6) for given surfaces, and other settings.

After entering the parameter settings, the user can select the lattice structure type from a set of pre-defined types. In the surface selection stage, the class selection dialog is loaded that makes selection for only surfaces in the current working part. After selecting the surface, the

Figure 7: Interface flow chart

user can choose what direction to add the lattice structure. Arrows appear that indicate the normal direction in which the lattice structure will be added; the direction can be flipped by selecting the surface that user wants to change. TrussCreator generates lattice structures based on input information mentioned above. After generating the lattice structure, it is displayed with its parent surfaces in the NX system. The user can examine the lattice structure details using NX functionality and save the structure as an STL file. Capabilities are offered to edit the lattice structure (add/modify/delete nodes and edges). Additionally, structural analysis or optimization can be performed by exporting files for input into ANSYS.
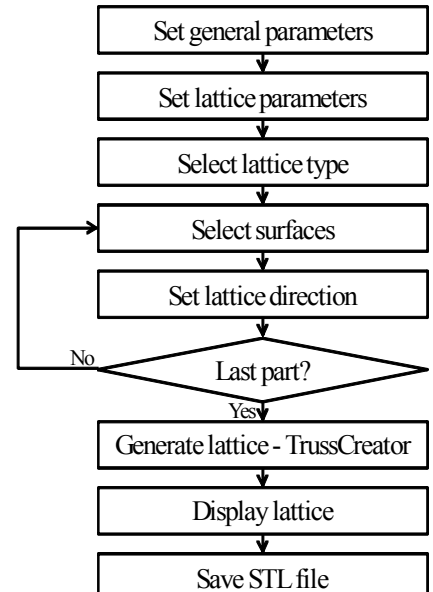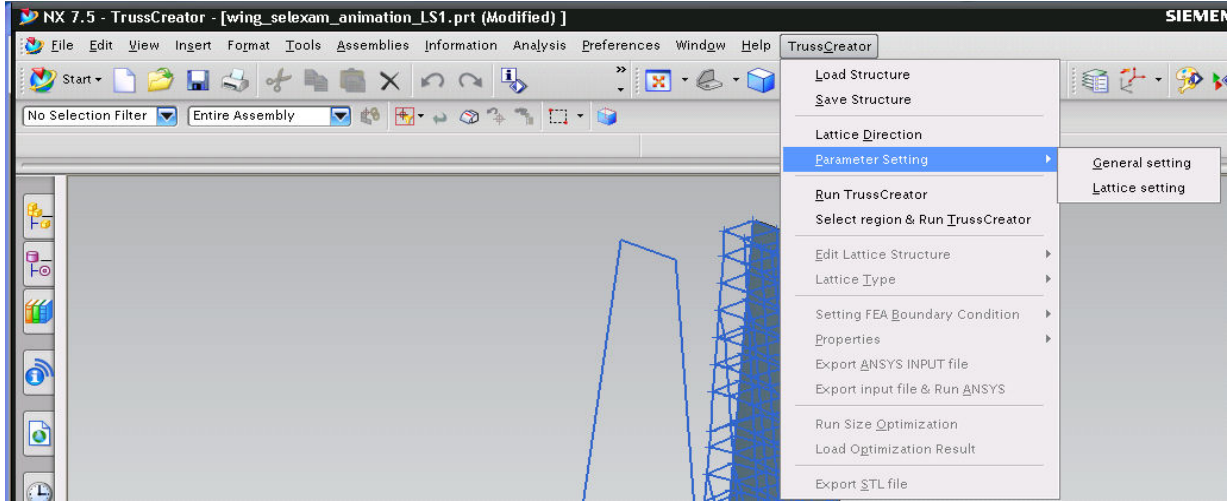
144

Figure 8.   TrussCreator menu.

3   Augmented Size Matching and Scaling (SMS) Method

Regardless of which structural optimization approach outlined in Section 1.4 is used for the design of meso-scale lattice structures (MSLS), an actual multi-variable optimization routine must be performed. Since the computational complexity of the design problem often scales exponentially with the number of design variables, topology optimization is infeasible or impractical for large design problems. The Size Matching and Scaling (SMS) method uses a heuristic to reduce the multivariable optimization problem to a problem of only two variables [22]. The heuristic is based on the observation that the stress distribution in a MSLS will be similar to the stress distribution in a solid body of the same overall shape. Based on the computed local stress states from the solid body analysis, unit cells from a predefined unit-cell library are selected and sized to support those stress states. The optimal diameters of these struts are then computed by performing a two-variable optimization. This design approach removes the need for a rigorous multi-variable topology optimization, which is a main bottleneck in designing MSLS.   The previous SMS method [22] was limited to MSLS designs with simple geometry and shape because of the lack of systematic ground structure generation capability. To overcome this limitation, the new augmented SMS method presented here integrates the CLS construction methods outlined in Section 2 to the ground structure generation process of the SMS method.

3.1   Problem Formulation

Each meso-scale lattice structure design problem has its own loading condition, geometric properties and desired performance specification. However, they can all be characterized as multi-objective design problems using the Compromise Decision Support Problem (cDSP) method [23].   The specific problem formulation for the SMS method is presented in Table 1.

The symbols p^{BG}, p^{F}, p^{M} represent the boundary, loading and material properties, respectively. The strut diameter, D_i, can either range from the lower diameter bound, D_{LB}, to the upper diameter bound, D_{UB}, or zero.   The symbol σ_i represents the axial stress value in each i strut. The symbols V and d represent the volume and the deformation of the structure. W_d and W_V represent weighting variables for d and V in the minimization function, Z. The volume of the structure is calculated by summing the volume of all the struts in the structure, which are assumed to be cylinders:

$$V = \sum \pi \times \frac{D_i^2}{4} \times l_i \qquad\qquad (1)$$

where D_i and l_i represent the diameter and length of each of the i strut in the structure. In this calculation, the overlapping volumes where the struts meet are not subtracted from the overall volume of the structure because they are assumed to have negligible contributions in order to simplify the calculation. The symbols i, j, and k represent each unit-cell region in the structure, each unit-cell configuration in the unit-cell library, and the strut number in each of the j configurations in the library, respectively; n represents the nodes from the solid-body finite element analysis.

Table 1: Mathematical cDSP formulation for the SMS design problem [22]

Given:	$p^{BG}, p^{F}, p^{M}, p^{UC}, \; S_{i,j}^{L}, \; i, k$	
Find:	$D_{i,k} = S_{i,j}^{u} \times S_{i,j}^{L} \times (D_{MAX} - D_{MIN}) + D_{MIN}$	(a)
	D_{MAX}, D_{MIN}	(b)
	$S_{i,j}^{u} = \dfrac{\sum \sigma_n - \sigma_{i,j}^{\min}}{\sigma_{i,j}^{\max} - \sigma_{i,j}^{\min}}$	(c)
Satisfy:	$D_{LB} \le D_{MIN} \le D_{MAX} \le D_{UB}$	(d)
	$\sigma_i \le \sigma_{max}$	(e)
	$V \le V_{max}$	(f)
Minimize:	$Z = (W_d \times d)^2 + \left(W_V \times \dfrac{V - V_t}{V_t} \right)^2$	(g)

The SMS method requires additional information besides the starting topology, and the boundary condition. External sources of information include the unit-cell library and the solid-body finite element analysis. Using that information, the determination of the strut diameters, shown in (a) of Table 1, reduces to a 2-variable optimization problem. It can be seen that $D_{i,k}$ can be determined using the pre-scaled maximum and minimum diameter value, D_{MAX} and D_{MIN}, a stress scaling factor from the unit-cell library, $S_{i,j}^{u}$, and a unit-cell scaling factor from the solid-body stress analysis, $S_{i,j}^{L}$. Hence, only D_{MAX} and D_{MIN} need to be determined through optimization. The minimization function, (g) of Table 1, is formulated in the least-squares format to minimize the deflection of the structure, d, and deviation of the structural volume from a target volume, V_t. W_d and W_V represent the weighting variables for d and V.

The optimization process of D_{MAX} and D_{MIN} requires calculation of deflection, volume, and associate stresses using finite element analysis of the truss structure. The finite-element package, which assumes each truss member as a beam element, was developed in MATLAB [24]. Once the optimization is done, the diameter of each strut is obtained using Equation (a) of Table 1. The optimized maximum and minimum diameters of the structure are denoted as D_{max} and D_{min} to differentiate from the pre-scaled maximum and minimum diameter value, D_{MAX} and D_{MIN}. It is important to note that the finite element analysis of the truss structure is conducted using the scaled/true diameters of the structure. Other problem formulations with different objective functions can also be used with the SMS method.

3.2   Overview of Augmented SMS method

The SMS method can be divided into eight discrete tasks that are completed in seven steps, as summarized in Figure 9.   Outputs of each step are shown in the shaded box under each step.

3.2.1 Step 1: Specification of loading, boundary conditions and material properties

In this first step of the method, the boundary conditions, material properties, and loading conditions are specified for the target meso-scale lattice structure. These properties will be utilized to perform the stress analysis of both the solid-body representation in step 2b and the

Figure 9: Overview of augmented SMS method

truss structure during the optimization process of step 7.   These values include the material properties such as Poisson's ratio, Young's modulus of elasticity, and the desired loading and boundary conditions.

3.2.2 Step 2a: Generation of ground structure

In this step of the method, the ground structure of the MSLS is created.   The ground structure only specifies the bounding geometry of the truss structure and contains no actual struts or materials.   In this implementation of the SMS method, a free mesh approach is utilized to generate the ground structure that conforms to an arbitrary complex surface.   Computer-aided technologies were developed for efficiently generating and representing the lattice structure [25], as described in Sec. 2.2.

3.2.3 Step 2b: Solid body finite-element analysis

A solid body is generated that envelopes the part model surfaces and the MSLS and a stress analysis is performed using finite-element analysis. The loading and boundary condition, and material properties for the structural analysis are specified in step 1 of the method.   The purpose of this step is to obtain the stress distribution of the solid-body structure and extrapolate this information to determine the stress distribution and the local stress states in the MSLS.   Once the analysis is complete, the von Mises stress distribution of the structure is obtained.   The primary deliverable of this step is the general state of stress at each node, which is characterized by six independent normal and shear stress components, σ_{xx}, σ_{yy} σ_{zz}, τ_{xy}, τ_{xz}, and τ_{yz}.

3.2.4 Step 3: Map FEA nodes to ground structure

In order to use the finite-element analysis result obtained from step 2b, the stress results must be appropriately mapped to the ground structure. The goal of this step is to determine which finite-element nodes correlate to which unit-cell region in the ground structure.   Since
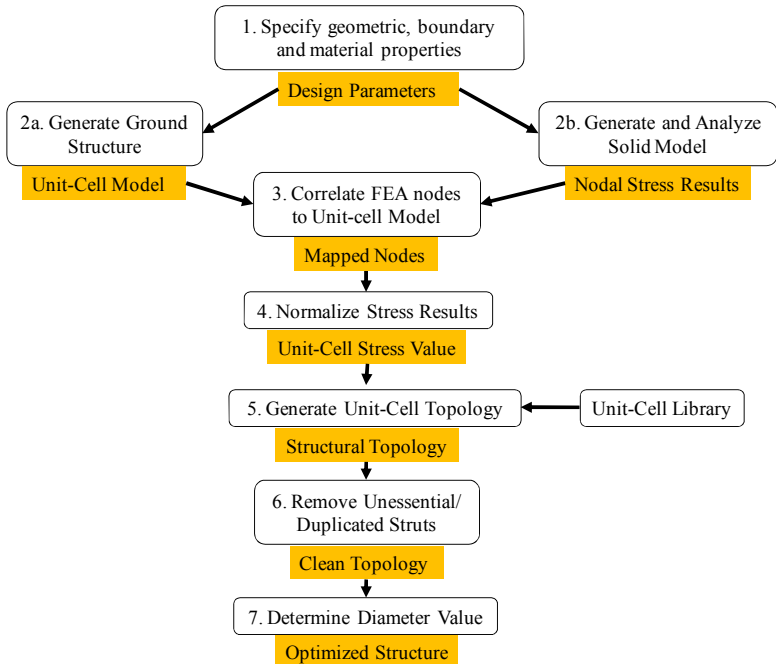
147

the free mesh approach is utilized to generate the ground structure, the augmented SMS method requires a FE node classification method that works with arbitrarily shaped mesh elements.

The process starts by dividing each face of the unit cell into triangles, since triangles are convex and planar, and every polygon can be broken up into a set of triangles. An outward-pointing normal for each triangle can then be obtained by computing the cross-product of two of the edges. After all the normal vectors are obtained for the unit cells, we can determine whether or not a finite-element node falls into the unit cell by computing the dot-products between the triangle normal vectors and the vector from a vertex of each triangle to the node. For hexahedra mesh elements, there will be a total of twelve triangles with twelve outward-pointing normals and twelve dot product operations. If and only if all the dot product results are either 0 or less than 0, then the finite-element node belongs to that unit cell. In the case that one of the dot products is equal to 0, the finite-element node is on the boundary between multiple unit cells and will be included in each. After the node mapping process is done, each unit cell will contain a list of finite element nodes that will be included in the calculation of the stress distribution in that unit cell.

3.2.5   Step 4: Stress Scaling and Normalization

After step 3 is complete, the stress values from the finite-element nodes in each unit cell are averaged to determine average stress values of six independent normal and shear stress components. Only the absolute values of the stresses are averaged. The stress results from FEA are only relevant for the solid-body structure. Instead, the stress distribution is of interest and will be used to guide the setting of strut sizes. Therefore, the stresses are normalized from zero to one such that the largest value of stress is equal to one. These six scaling values correlate to six entries of each configuration in the unit cell and will be utilized to size the struts during the topology generation process in step 5.

In topology generation, the diameter values of the selected unit-cell configuration from the preconfigured unit-cell library are scaled against the associated stress values (σ_{xx}, σ_{yy}, σ_{zz}, τ_{xy}, τ_{xz}, and τ_{yz}) and then mapped to the unit cells in the ground structure. However, since the solid-body results are provided relative to the global coordinate system, stress transformations are needed to ensure correct topology generation, which is performed by rigid-body rotation of the axes. However, since the unit cell is not necessarily a cuboid hexahedron, a representative local coordinate system can be determined using the following approach. Each unit cell, such as in Figure 10, from the ground structure is characterized by 8 nodes and 12 edges. Three edges of the unit cell, edge 1-2, edge 1-4, and edge 1-5, respectively, are selected as reference edges, nominally representing the x, y, and z axes, respectively. For each edge that corresponds to the direction of a certain axis, the angle between that edge and the corresponding reference edge is calculated; e.g. in the x-axis direction, the angles between edge 1-2 and edge 5-6, edge 1-2 and edge 8-7, and edge 1-2 and edge 4-3 are calculated and averaged. This step is repeated for the other two directions. The reference edge with the lowest average angle is selected as the starting axis for that particular direction.   The reference edge with the second lowest average angle is selected as a second axis. The cross product is performed between the first and second axes to find the third orthonormal axis. Then another cross product is computed between the third and first axes gives the second orthonormal axis. This approach determines the local orthonormal coordinate system of a unit cell from the ground structure.
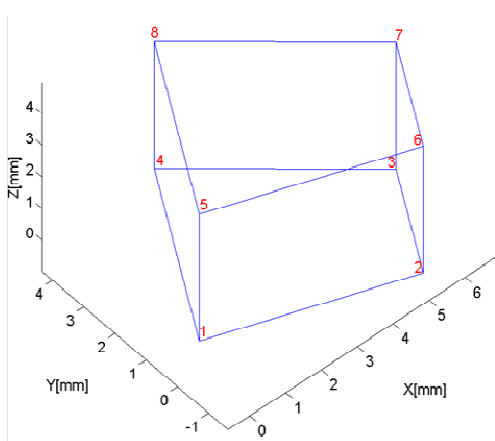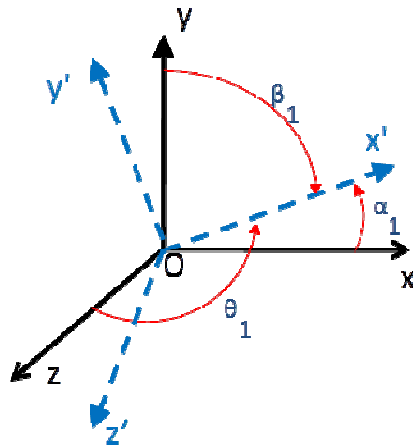
Figure 10: Unit-cell region

Figure 11: Rotation of coordinate system (x', y', z')

After obtaining the local coordinate system for the unit cell, the relative orientation between the local and global coordinate system can be determined. The global coordinate system, xyz, and local coordinate system, x'y'z', are shown in Figure 11 where α_1 is the angle between the x' and x axes, β_1 is the angle between x' and y axes, θ_1 is the angle between x' and z axes, α_2 (not shown) is the angle between the y' and x axes, and so forth.

Let R be the rotation matrix that transforms the vector components in the original coordinate system to those in the primed system, then

$$\begin{Bmatrix} x' \\ y' \\ z' \end{Bmatrix} = \begin{bmatrix} R_{11} & R_{12} & R_{13} \\ R_{21} & R_{22} & R_{23} \\ R_{31} & R_{32} & R_{33} \end{bmatrix} \begin{Bmatrix} x \\ y \\ z \end{Bmatrix} \tag{2}$$

From Eqn. 2, it can be seen that the unit vector x' can be expressed in the original coordinate system as

$$x' = R_{11}x + R_{12}y + R_{13}z \tag{3}$$

where R_{ij} are direction cosines. Therefore, x' can be expressed in terms of x, y, z using Eqn. 4.

$$x' = \cos(\alpha_1)x + \cos(\beta_1)y + \cos(\theta_1)z \tag{4}$$

Similarly, axes y' and z' can be expressed in term of $x, y,$ and z. In matrix form, the coordinate transformation is shown in Eqn. (7).

$$\begin{Bmatrix} x' \\ y' \\ z' \end{Bmatrix} = \begin{bmatrix} \cos(\alpha_1) & \cos(\beta_1) & \cos(\theta_1) \\ \cos(\alpha_2) & \cos(\beta_2) & \cos(\theta_2) \\ \cos(\alpha_3) & \cos(\beta_3) & \cos(\theta_3) \end{bmatrix} \begin{Bmatrix} x \\ y \\ z \end{Bmatrix} \tag{5}$$

The stress state at a point P is characterized by six independent normal and shear stress components, as shown in Figure 12. These components can be organized into a matrix:

$$\begin{bmatrix} \sigma_{xx} & \tau_{xy} & \tau_{xz} \\ \tau_{yx} & \sigma_{yy} & \tau_{yz} \\ \tau_{zx} & \tau_{zy} & \sigma_{zz} \end{bmatrix} \qquad (6)$$

The grouping of these stress components becomes the components of a second-order stress tensor. This stress tensor is defined in the deformed state of the material and is known as the Cauchy stress tensor [26]. With the rotation matrix given in Eqn. 5, the Cauchy stress tensor in the local coordinate system (x', y', z') can be obtained using Eqn. 7.

$$[\sigma'] = R[\sigma]R^T \qquad (7)$$

R^T is the transpose of R, σ is the Cauchy stress tensor in global coordinate system (x, y, z), and σ' is the Cauchy stress tensor in the local coordinate system (x', y', z'). This follows the rule of changing second-order tensor components under rotation of axes [26]. Ultimately, there will be six stress values for each unit cell, σ_{xx}, σ_{yy} σ_{zz}, τ_{xy}, τ_{xz}, and τ_{yz}, which correspond to the scaling factors, $S_{i,j}^u$, in (a) of Table 1.

3.2.5 Step 5: Topology generation

The unit-cell lattice structure selection and mapping process will be described in detail in Section 3.3. After this step is complete, the structure will have a topology designed for the anticipated stress distribution in the truss structure. The relative thickness of one strut to another is known. However, these normalized diameters must be correlated with actual strut diameter values in step 7 of the method.

Figure 12: General state of stress [26]

3.2.6 Step 6: Ambiguity resolution

Since the unit cells are populated individually, there will be instances of overlapping struts between adjacent unit cells. These struts will have identical start and end nodes. To resolve this ambiguity, the largest diameter strut is kept and all other smaller struts are removed. Duplicated nodes are also removed.

3.2.7 Step 7: Diameter Sizing

The normalized strut diameters must be replaced with the actual diameter values to satisfy the loading and volume condition. It can be seen from the problem formulation for the SMS method shown in Table 1, the only parameters missing to determine the diameter of each strut are the D_{MIN} and D_{MAX}, where D_{MAX} and D_{MIN} correspond to pre-scaled thickest and thinnest diameters, respectively. After D_{MIN} and D_{MAX} are calculated, the diameters of each strut can be determined using Eqn. 8.

$$D_{i,k} = S_{i,j}^u \times S_{i,j}^L \times (D_{MAX} - D_{MIN}) + D_{MIN} \qquad (8)$$

where $D_{i,k}$ is the diameter value of the kth strut in the ith unit cell.

In the 2-variable approach, values D_{MIN} and D_{MAX} are determined by performing 2-variable minimization of the objective function (g) from the problem formulation in Table 1. It is rewritten in Eqn. 9 as a function of both D_{MIN} and D_{MAX}, where $V(D_{MIN}, D_{MAX})$, volume, and $d(D_{MIN}, D_{MAX})$, deformation, are functions of only D_{MIN} and D_{MAX}. Deformation, d, represents any
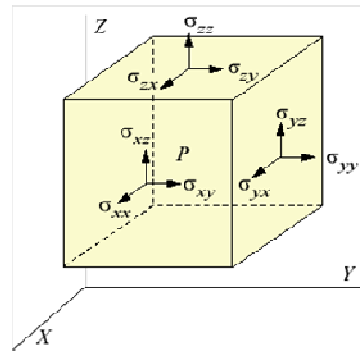
150

unit of measure that is directly proportional to structural stiffness, such as tip deflection or strain energy. The target structure must attempt to minimize both volume and deflection. However, these two goals have competing effects. The target deflection is usually set to zero. Two algorithms used to perform this two-variable minimization are the Levenburg-Marquardt and active-set algorithms. The Levenburg-Marquardt algorithm has documented success in design and optimization of MSLS [21], while the active-set algorithm is documented to have success in optimization of multivariable, nonlinear and constrained optimization problems [29].

$$Z(D_{MIN}, D_{MAX}) = (W_d \times d(D_{MIN}, D_{MAX}))^2 + \left(W_V \times \frac{V(D_{MIN}, D_{MAX}) - V_t}{V_t} \right)^2 \tag{9}$$

In addition to exploring the two-variable optimization approach, it was noted in previous research that for a particular truss structure there is an ideal relationship between D_{MIN} and D_{MAX} such that when the ratio is approximately equal to 28% for a specific target volume, the structure would have the least deflection [27]. This finding has significant effect because it would reduce the two-variable equation involving D_{MIN} and D_{MAX} to a one-variable equation. As a result, the equation to determine the diameter of each strut becomes:

$$D_{i,k} = \left[0.72 \left(S_{i,j}^u \times S_{i,j}^L \right) + 0.28 \right] \times D_{MAX} \tag{10}$$

In this research, both one-variable and two-variable approaches will be used. The results will be compared in terms of the deformation and design time.

3.3 Unit-cell Library

The second component of the augmented SMS method is the unit-cell library, which was developed to generate the topology for the MSLS [22]. There are seven different unit-cell configurations in the library. Each configuration has six entries with each specialized for six independent normal and shear stress components. Entries in the library were optimized for loading conditions corresponding to each of the six stress states.

3.3.1 The optimization process

The problem formulation utilized for the optimization of unit cells is shown in Table 2.

Table 2: Qualitative cDSP formulation for the optimization of unit cells [15]

Given:	Loading and Fixity Conditions, Starting Lattice Topology
Find:	Truss Diameters/Lattice Topology
Satisfy:	Target Strain Energy Maximum Stress Value
Minimize:	Volume

For unit-cell optimization, the objective is to minimize the volume of the unit cell. The stiffness is set as a constraint to force the performance of all the optimized unit-cells to be equal. Strain energy ΔU, is the metric to measure stiffness, which is calculated as:

$$\Delta U = \frac{\Delta F}{2} d \tag{11}$$

where $\frac{\Delta F}{2}$ is the average magnitude of the load and d is the total displacement of the structure. Strain energy is widely used in topological optimization problem.

The optimization process for the unit cell is divided in to five separate steps as described below.

Step 1: Insert Initial Unit-Cell Configuration: Each unit cell is defined in a cuboid region by 8 nodes in each corner.   A diameter value of "1" is assigned to all the struts in the unit cell.

Step 2: Apply Loading Conditions: In this step, the unit cell is loaded with six loading conditions, each for a component of the stress state.   The loading conditions are shown in Figure 13.

These loading conditions must be applied in multiple directions.   For instance, there are 4 shear directions in the XY plane including τ_{xy}, $-\tau_{xy}$, τ_{yx}, $-\tau_{yx}$. The unit-cell must be optimized individually for each direction and then combined to form the final optimized unit-cell.

Figure 13: Loading conditions for unit-cell optimization [22]

Step 3: Optimize unit-cell: After defining the base-lattice structure and loading conditions, the unit-cell was optimized using the parameters in Table 3.   The analysis and optimization was done in ANSYS 13. 0

Step 4: Combine Optimized Unit-Cells: Since the loading conditions are applied in multiple directions, the results from each direction must be combined to form an optimized unit cell. The process is illustrated in Figure 14 for shear stress in the XY plane.   When combining the results, the largest diameter for each strut is kept and all other instances are deleted.

After all the configurations are optimized, the diameters of the unit cells are normalized from 0 to 1:

Table 3: Optimization parameter for unit-cell optimization in ANSYS[22]

$$D_{j,k,l}^{norm} = \frac{D_{j,k,l}}{D_l^{max}} \qquad (12)$$

Strain Energy Constraints (mJ)	50
Poisson Ratio	0.3
Elastic Modulus (N/mm2)	1960
Loading Magnitude (N)	10

where j represents each strut for each kth configurations for each of the l stress directions. k goes from one to seven because there are seven configuration. l goes from one to six because there are six stress directions, σ_{xx}, σ_{yy}, σ_{zz}, τ_{xy}, τ_{xz}, and τ_{yz}.   Hence, D_l^{max} represents the largest diameter value among the six stress directions. $D_{j,k,l}^{norm}$ becomes the unit-cell library scaling factor that is used in the diameter determination step.

After the normalization process is complete, the unit-cell library is stored in a list with three key parameters: the nodal coordinates, the elements, and the diameters of each element

3.3.2 Unit-cell selection

One way to generate the best topology for the structure is to iteratively populate each unit cell in the ground structure with a configuration from the library and analyze the performance of the structure. However, it is computationally infeasible because there are M^N number of possible combinations of topology where M is the number of configurations in the unit-cell library and N is the number of unit cells in the ground structure. For instance, a ground structure with 5 unit
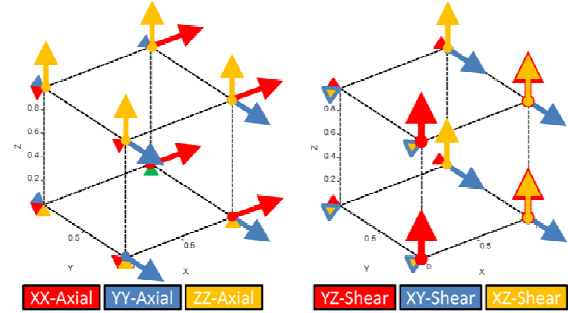
cells would already have $7^5 = 16807$ unique topologies. Therefore, a heuristic was developed for the selection process.

Since all the configurations of the unit-cell library are optimized such that they have identical performance, the structure with the smallest normalized volume is selected. The selection is performed using the Equation (18) [22], which incorporates three terms. The first is the sum of all lattice structure unit-cell volumes from the 6 stress states. The second term is the volume of the structure if it were mapped into the particular mesh element, while the third term represents a

Figure 14: Combination of optimized unit-cells for shear stress in XY plane for Cantley configuration [22]

performance term based from empirical results. This term attempts to predict how well a configuration will perform when multiple instances of the configuration are utilized.

This selection process is performed for each unit cell from the ground structure and the configuration with the lowest rating, r, is selected for that unit cell.

$$r = W_v \times \sum V_\sigma + W_{vn} \times V_{net} + W_p \times \sum P \qquad (13)$$

where

$$\sum V_\sigma = V_{xx} + V_{yy} + V_{zz} + V_{xy} + V_{xz} + V_{yz} \qquad (14)$$

$$\sum P = P_{xx} + P_{yy} + P_{zz} + P_{xy} + P_{xz} + P_{yz} \qquad (15)$$

and W_v, W_{vn}, and W_p are weights (importances) on each term.

For each topology configuration, the volume of each entry in six primary stress directions (σ_{xx}, σ_{yy}, σ_{zz}, τ_{xy}, τ_{xz}, and τ_{yz}) is multiplied by the corresponding normalized stress results from step 4 of the SMS method and then summed to determine $\sum V_\sigma$ as shown in Eqn. 14. For each topology configuration, $\mathbf{V_{net}}$ is the net volume of each configuration calculated by combining all six entries in six stress direction and removing the overlapping struts. $\sum P$ for each topology configuration is determined, as shown in Eqn. 15, using a performance table. These values are provided in Table. They are determined using results from a design example [22]. In this example, a 15 × 15 × 15 cm cube is divided into 3 × 3 × 3
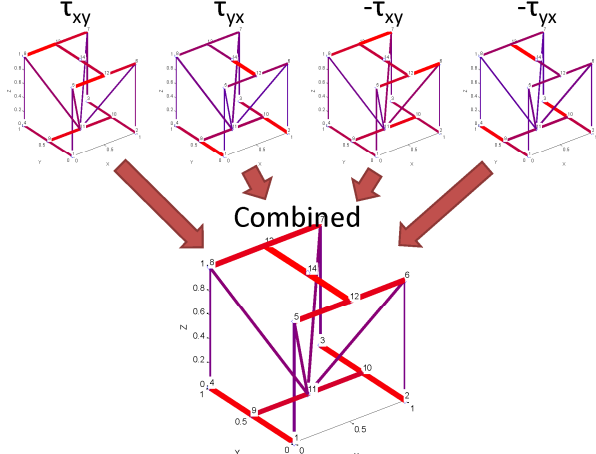

Figure 15: Unit-cell library [22]

153

of the same unit-cell configuration. The same loading and boundary condition, shown in Figure 13, is applied to the cube. There are six loading condition approximating the six axial and shear stresses. Each of these loading conditions will be applied to all seven configurations in the library; therefore, there will be 42 unique topologies, as shown in Figure 15. The strain energy from each topology is calculated. The results are normalized between 0 and 1 and plugged in the performance table to calculate $\sum P$. In addition, there are three weighting values W_v, W_{vn}, and W_p, which can be set manually to vary the importance of each contributing factors to generate different topologies. The configuration with the lowest rating is selected and mapped to that particular unit cell in the ground structure.

Table 4: Performance table used for selection of unit-cell configuration [22]

	XX Axial	YY Axial	ZZ Axial	XY Axial	YZ Axial	XZ Axial
Crossed	0.0745	0.0693	0.0375	0.0810	0.0747	0.0752
Cantley	0.5399	0.4885	0.0539	0.5418	0.5353	0.2626
Octet	0.2281	0.2023	0.1050	0.1004	0.0891	0.0863
Paramount1	0.0197	0.0907	0.0500	0.9865	0.3904	0.3734
Diagonal	0.0743	0.0704	0.0390	0.1166	0.0881	0.0956
Paramount2	1.0000	1.0000	1.0000	0.6043	0.5569	0.5462
Midpoint	0.1058	0.0955	0.0507	1.0000	1.0000	1.0000

3.3.3 Mapping

Once the best possible configuration is determined for a unit cell in the ground structure, it is mapped to that region. If there is a node from the unit-cell configuration that does not exist in the unit cell of the ground structure, it will be added using 3-D linear interpolation. After all the missing nodes are added, the unit-cell configuration can then be populated into the unit cell. The normalized stress values from step 4 of the augmented SMS method are scaled against the normalized diameter values from the unit cell library to determine the relative thickness of one strut to another.

4 Design Examples

In order to validate the augmented SMS method, it will be applied to three design example. The first example is a 3-D curve cantilever beam. The second example is a micro aerial vehicle fuselage. These examples serve to validate the augmented SMS method and demonstrate its ability to design large-scale MSLS on complex-shaped parts with curve or non-rectangular surfaces.

4.1 Curved Cantilever Beam

The first example is a simple, three-dimensional, curved cantilever beam with rectangular cross section. The beam is fixed at one end and has two point loads applied in the z-direction at the free end. The initial properties of this design problem are provided in Table 5. Ultimately, the primary goal of this example is to illustrate the modified algorithm in steps two, three, and four has allowed the augmented method to overcome the significant limitations with the previous

implementations of the SMS method which cannot be utilized in structures with curved surfaces. For this example, the unit-cell regions do not have local coordinate systems that are the same as the global coordinate system. The weighting values from Eqn. 13 are set at: $W_v = 1$, $W_{vn} = 1$, $W_p = 0$. With these values, the topology was generated with 28 diagonal configurations. Other topologies were also generated by varying the weighting values. However, this topology has the best structural performance for this particular structure and loading condition. Figure 16 shows the final topology of the curved cantilever beam using active-set method, as well as the results from the intermediate steps. The strut diameter results are summarized in Table 6. The results show that the 28% method is able to converge about 6 times faster than either two-variable optimizations; however, the deflection result is worse than either two-variable approaches. The two 2-variable optimizations return identical results. However, the active-set method is able to converge faster. As mentioned in example 1, it is important to note that the diameter results reported for the SMS method are the actual diameters of the structure after being scaled against the solid body analysis and unit cell library scaling factors. The pre-scaling D_{MIN} and D_{MAX} for the active set method are 0.4135 mm and 7.0704 mm, respectively.

Table 5: Initial properties of the curve cantilever beam

Outer Radius (mm)	84.5
Inner Radius (mm)	74.5
Width (mm)	20
Length(mm)	105
Loading Magnitude (N)	1
Elastic Modulus (N/mm^2)	1960
Unit-cell size in-plane (mm)	10
Unit-cell size out-plane (mm)	10
Target Volume (mm^3)	5000

Besides the three optimization approaches, a design space exploration/grid search was conducted. The design space exploration is done using pre-scaling values of diameters. This was performed by iterating both D_{MIN} and D_{MAX} from 0.1 to 10 mm with increments of 0.1 mm. The result is plotted in Figure 17. Based on the results from the initial exploration, a finer resolution of the design space was conducted around the apparent minimum by searching D_{MIN} from 0.3 to 0.5m and D_{MAX} from 6.9 to 7.3 mm. with increments of 0.01 mm, as shown in Figure 18. The red diamond indicates the minimum found in design exploration. Diameter results that return the lowest objective function value are shown in Table 6. The pre- and post-scaling values from the design space exploration are included in two of the columns. These diameter values are found to be close to the values obtained from the SMS method. Both two-variable optimizations were able to return results with much lesser design time than the design space exploration.

In addition to the augmented SMS method, ground truss approach was utilized to perform topology optimization for this selection scenario. Levenberg-Marquardt algorithm was used to optimize the ground truss. When compared with the ground truss approach, the augmented SMS has comparable performance result, but is able to converge much more quickly with about 70 times decrease in design time using two-variable approach and about 400 times decrease in design time using one-variable approach

4.2 Micro Aerial Vehicle (MAV) Fuselage

The final design example is a micro aerial vehicle (MAV) fuselage. MAVs play a critical role in modern military operations as they allow easy surveillance in hazardous environment. The next generation of these aerial robotic systems needs to have enhanced take-off and landing capabilities, better endurance, and be adaptable to mission needs in varying conditions [28]. In

terms of the design of the wings and fuselage of these MAVs, some types of structures and/or materials that are lighter, stronger and customizable are highly desired.
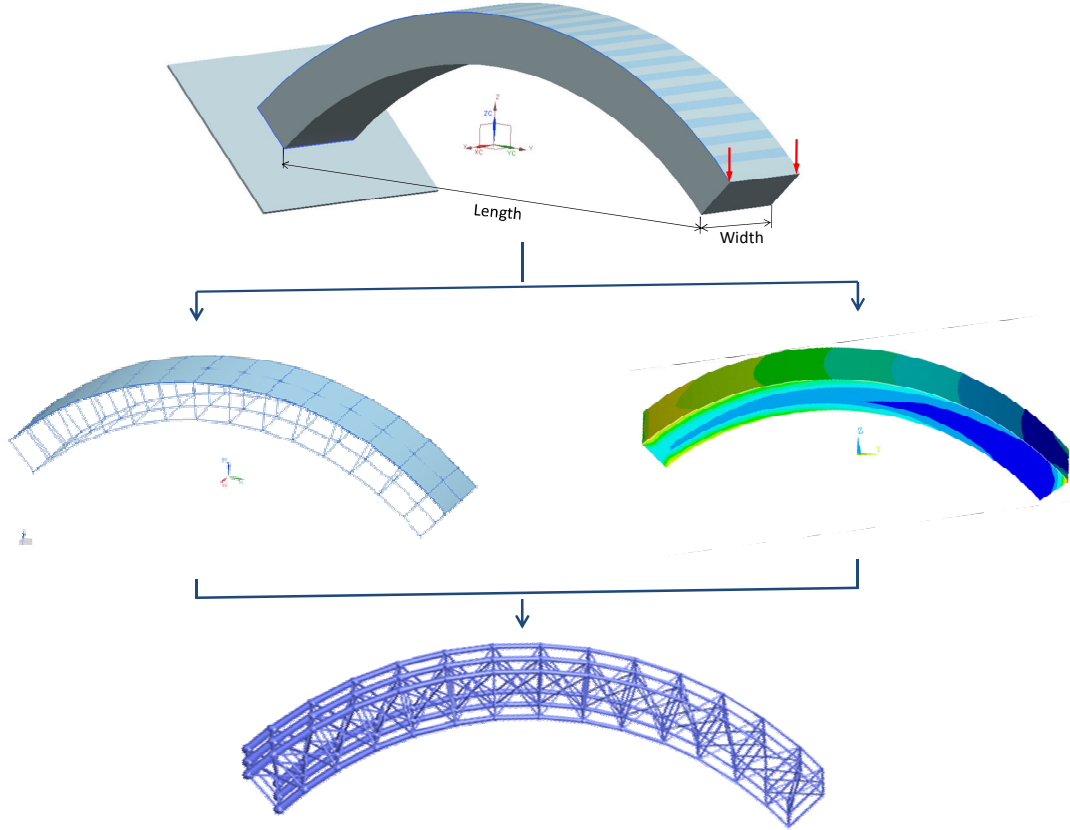

Figure 16: Final topology of curved cantilever beam using active-set method

Table 6: Optimization result for the curved cantilever beam

Optimization Approach	SMS 28% Assumption	SMS Active-Set	SMS Least-square Minimization	SMS Design Space Exploration (Pre-Scaled)	SMS Design Space Exploration Scaled	Ground Truss LM
Deflection(mm)	1.341	0.901	0.901	0.900	0.900	0.780
Volume (mm³)	5501.0	5500.5	5500.5	5500	5500	5501
D_{min} (mm)	1.13	0.65	0.65	0.41	0.64	--
D_{max} (mm)	2.43	3.88	3.88	7.09	3.87	--
Design Time (s)	7.8	46.7	52.8	2860	2860	3260

In this design example, the fuselage is designed to withstand the impact when landing or crashing. There is a distributed load from the payload applied to the inner surface of the fuselage. The weight of the motor and the tail are modeled as point loads at their centers of mass. This is done in ANSYS using a rigid link element. The equivalent couple is applied to the truss structure. All these weights are scaled by a factor of ten to simulate impact when crashing. The weight of the wing is small and assumed to have negligible contribution. A small area on the bottom of the fuselage is fixed to model the contact zone as the MAV is crashing. Multiple

views of the fuselage are shown in Figure 19 with key dimensions labeled. The initial properties of the design problem are provided in Table 7.
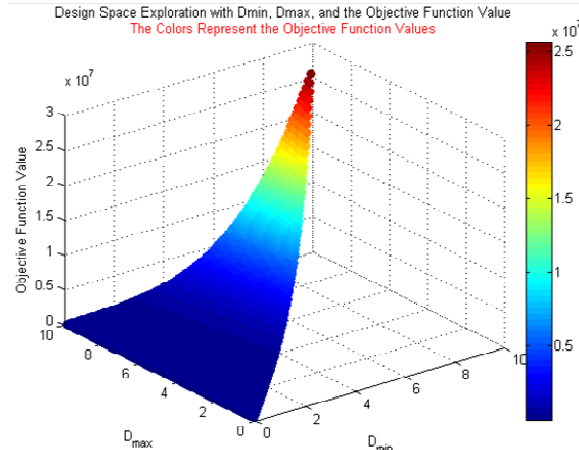

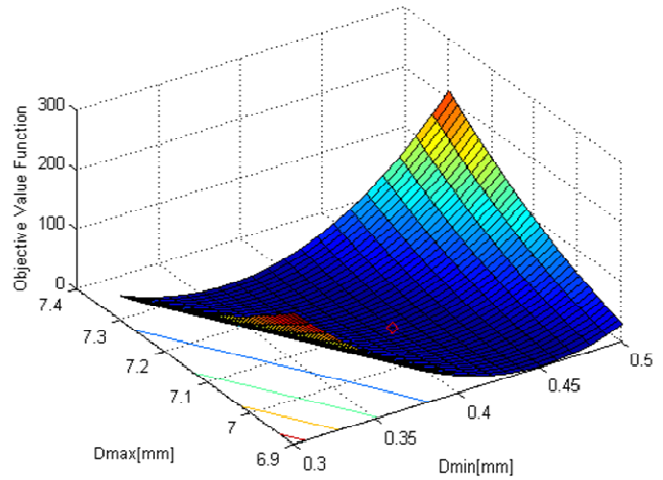Figure 17: Design space exploration for the curved cantilever beam

Figure 18: Design space exploration with finer resolution around the solution for the curved cantilever beam

Table 7: Initial properties for the fuselage

A1 (mm)	47	L (mm)	254
A2 (mm)	90	Fmotor (N)	5.9
A3 (mm)	45	F$_{Tail}$ (N)	2.7
D (mm)	45	Fpayload (N/mm2)	0.1
Unit-cell in-plane (mm)	12	Modulus (N/mm2)	1960
Unit-cell in-plane (mm)	12	Poisson Ratio	0.3
Unit-cell out-plane (mm)	8	Target Volume (mm2)	100,000

The objective is to achieve a target volume of 100,000 mm^3 or 65% porosity relative to the solid model while minimizing the deflection of the structure. The ground structure for the fuselage is generated by TrussCreator with the desirable unit-cell sizes as provided in Table 7. There are 214 unit cells in the ground structure. The weighting values in Eqn. 13 set at: $W_v = 0$, $W_{nv} = 1$, $W_p = 5$. With these weighting values, the topology is generated with 101 crossed configurations and 113 diagonal configurations. The topology matches the expectation based on the solid-body analysis. Other topologies were also generated by varying the weighting values. However, this topology has the best structural performance for this particular structure and loading condition. The average displacement of selected nodes on the top of the fuselage, where the large displacement occurs according to the solid-body analysis, is used as the metric for deflection.

The strut diameter results are summarized in Table 8. The active-set method returns the best deflection value but at the expense of design time with more than four times longer than the fastest method: 28% assumption.

Figure 19: Multiple views of the fuselage

However, 28% assumption returns the worst deflection result compared to the two 2-variable approaches. Of the 2-variable optimization methods, the least-squares minimization approach
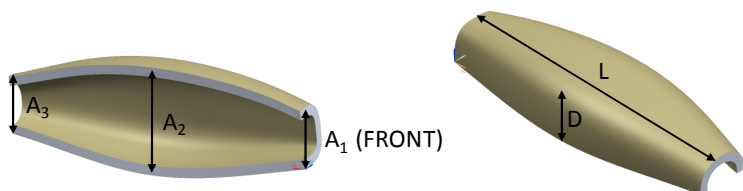
is noticeable faster. The structure contains 101 crossed configurations and 113 diagonal configurations. The pre-scaled values of D_{MIN} and D_{MAX} for the active set method are 0.5178 mm and 7.1406 mm, respectively. Figure 20 shows the final topology of the MAV design using the active-set method, as well as the results from the intermediate steps.
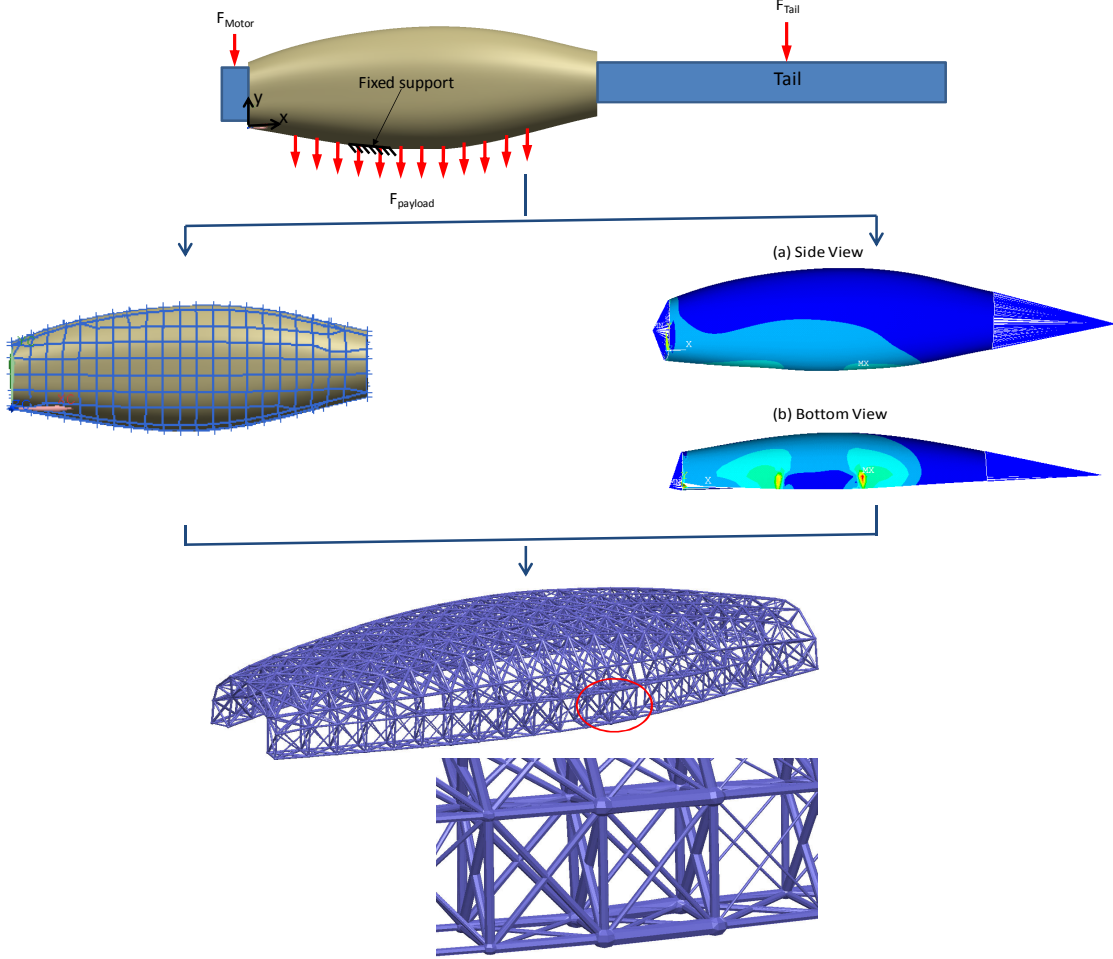

Figure 20: Final topology for the fuselage.

In addition to the three optimization approaches, design space exploration/grid search was conducted. The design space exploration is done using pre-scaling values of diameters. D_{MIN} and D_{MAX} were iterated from 0.1 mm to 10 mm and with an increment of 0.1 mm. The increment, 0.1 mm, is coarse to reduce analysis time. However, even with the coarse increment, the design space exploration already takes a long time to complete. Exhaustive search is not a feasible solution for structures with large numbers of struts. The result is plotted in Figure 21a. A finer resolution of the design space was conducted around the apparent minimum by searching D_{MIN} from 0.4 to 0.6 mm and D_{MAX} from 7 to 7.3 mm with an increment of 0.01 mm. Figure 21b shows the design space zoomed into the region of interest. The red diamond indicates the minimum found in the design space exploration. Diameter results that return the lowest objective function value are shown in Table 8. The design space exploration diameter values are found to be close to the values obtained from the SMS method. Both two-variable optimizations were able to return results with much less design time than design space exploration. It can be seen from

Figure 21b, there is a valley in the design space exploration near the solution, which might cause the active set method to converge slowly because of the shallow gradient along one direction.

Table 8: Optimization results for the fuselage

Optimization Approach	28% Assumption	Active-Set	Least-square Minimization	Design Space Exploration (Pre-scaled)	Design Space Exploration Scaled
Deflection(mm)	0.327	0.299	0.319	0.296	0.296
Volume (mm^3)	100000.0	99973.0	100010.0	100000	100000
D_{min} (mm)	0.85	0.65	1.12	0.48	0.62
D_{max} (mm)	3.04	4.16	3.29	7.28	4.22
Design Time (s)	378.6	1630.9	508.9	76660	76660

5. Conclusions

In this article, two advances are reported for designing MSLS. First, computer-aided design technologies were developed for efficiently generating and representing MSLS. More specifically, methods to construct conformal lattice structures were presented. Secondly, an augmented size matching and scaling design method for the design of conformal lattice structures was presented. This method enables us to design and efficiently optimize MSLS on complex-shaped parts by integrating the free-mesh approach in generating conformal lattice structures for the ground structure generation process. In addition, the method removes the need of rigorous large-scale multivariable topology optimization by utilizing a heuristic that reduces the multivariable optimization problem to a problem of only two variables, which combines solid-body analysis and predefined unit-cell library to generate the topology of the structure. Based on this work, the following conclusions can be made:

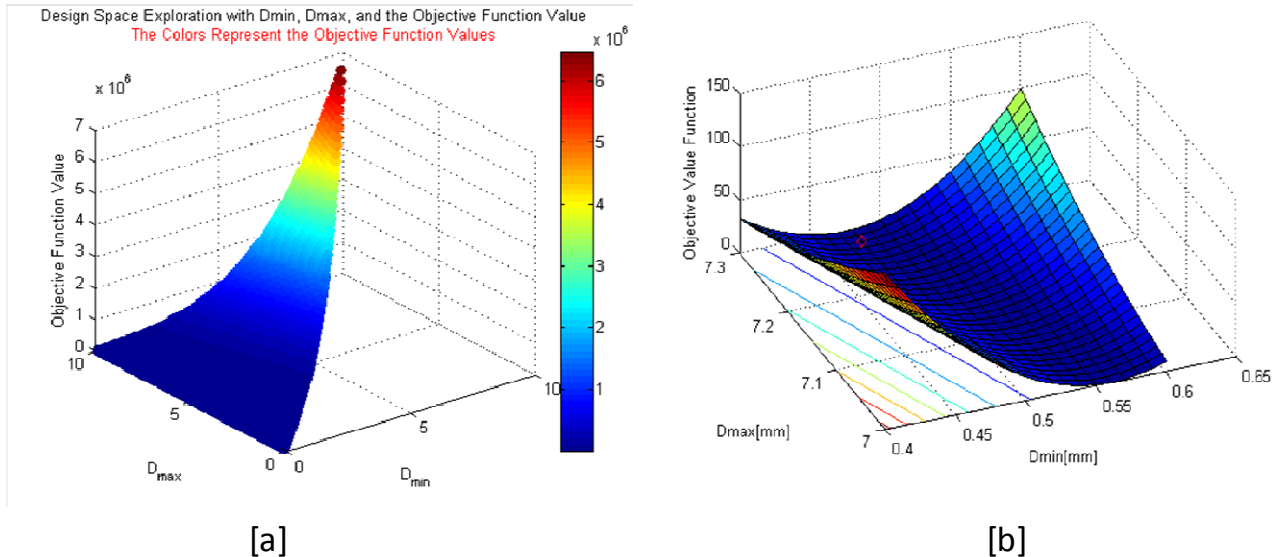[a]   [b]

Figure 21: [a] Design space exploration for fuselage, [b] Zoomed-in design space for the fuselage

- The present CLS construction methods produce lattice structures on a wide variety of surface shapes, demonstrating the generality of the method. These methods produced CLS that was of high quality, since the unit cells were of nearly uniform size.
- In step 3 of the augmented SMS method, a new algorithm was developed to determine which unit cell of the ground structure the finite-element nodes fall into. After the finite element nodes are mapped to the correct unit cells in the ground structure, a stress transformation from global to local coordinate systems of the unit cells is conducted using standard rigid-body rotations. Utilizing the property of second-order tensor, the stress was transformed to its proper local state to generate the correct topology as shown in the examples.
- For these particular structures with the given loading conditions, topologies generated with crossed configuration, diagonal configuration for Example 1, and a combination of cross and diagonal configurations for Example 2 return the best possible stiffness result.
- The weighting values W_v, W_{vn}, and W_p from Eqn. 13 should be set such that the topology is generated with the diagonal configuration for Example 1, and a combination of crossed and diagonal configurations in Example 2. These weighting values are associated with $\sum V_\sigma$, $\mathbf{V_{net}}$, and $\sum P$, respectively, in Eqn. 13. $\sum P$ is a performance parameter that always favors the cross configuration because it has the lowest strain energy.
- No generalized statement can be made on which unit-cell configuration should be selected because the method and the unit-cell library are only tested for a narrow set of design problems.
- Between one-variable and two-variable optimizations, one-variable optimization using the 28% assumption consistently returns diameter results much faster than either two-variable optimization methods, but at the cost of structure stiffness. The two two-variable optimization methods produced very similar results in the first design example in terms of stiffness and design time. However, least-squares minimization outperformed the active-set method in terms of design time in the MAV example. Due to the trade-off between design time and structural stiffness, the designer must make choose which design criteria are more important in his/her design when choosing the optimization approach.
- Overall, the augmented SMS method can be applied effectively in the design of conformal lattice structure with highly optimized stiffness and volume for complex surfaces. For simpler structures such as in Example 1, the augmented SMS method can reduce design time up to 70 times compared to normal topology optimization using a two-variable approach. In cases where topological optimization is infeasible, such as Example 2, the augmented SMS method can still effectively generate complex MSLS. This approach removes the need for a rigorous topology optimization, which is a main bottleneck in designing MSLS.

Acknowledgement

References
1. Rosen, D.W., *Computer-aided design for additive manufacturing of cellular structures.* Computer-Aided Design & Application, 2007. **4**(5): p. 585-594.
2. Gibson, I., D.W. Rosen, and B. Stucker, *Additive Manufacturing Technologies: Rapid Prototyping to Direct Digital Manufacturing.* 2010: Springer.
3. Gibson, L.J. and M.F. Ashby, *Cellular Solids: Structure and Properties.* 1997, Cambridge: Cambridge University Press.
4. Ashby, M.F., et al., *Metals Foams: A Design Guide.* 2000, Woburn, MA: Butterworth-Heinemann.

5. Deshpande, V.S., N.A. Fleck, and M.F. Ashby, *Effective properties of the octet-truss lattice material.* Journal of Mechanics and Physics of Solids, 2001. **49**(8): p. 1747-1769.

6. Wang, A.-J. and D.L. McDowell, *Optimization of a metal honeycomb sandwich beam-bar subjected to torsion and bending.* International Journal of Solids and Structures, 2002. **40**(9): p. 2085-2099.

7. Wang, A.-J. and D.L. McDowell, *Yield surfaces of various periodic metal honeycombs at intermediate relative density.* International Journal of Plasticity, 2005. **21**(2): p. 285-320.

8. Johnston, S.R., et al., *Analysis of mesostructure unit cells comprised of octet-truss structures*, in *Solid Freefrom Fabrication Symposium*2006: Austin, TX. p. 421-432.

9. Bendsøe, M.P. and O. Sigmund, *Topology Optimization: Theory, Methods and Applications.* 2003, Berlin: Springer.

10. Bendsøe, M.P., *Optimization of Structural Topology, Shape and Material.* . 1995, Berlin Heidelberg: Springer-Verlag.

11. Allaire, G., *Shape Optimization by the Homogenization Method.* 2002, New York: Berlin.

12. Pedersen, P., *On optimal shapes in materials and structures.* Structure Mutlidisciplinary Optimization, 2000. **19**: p. 169-182.

13. Rozvany, G.I.N., *Topology Optimization in Structural Mechanics.* 2003: Springer.

14. Michell, A.G.M., *Limits of economy material in frame structures.* Philosophy Magazine, 1904. **6**: p. 589-597.

15. Bendsøe, M.P. and N. Kikuchi, *Generating optimal topologies in structural design using a homogenization method* Computer Methods in Applied Mechanics and Engineering, 1988. **71**: p. 197-224.

16. Dorn, W., R. Gomory, and H. Greenberg, *Automatic design of optimal structures.* Journal Mechanica, 1964. **3**: p. 25-52.

17. Wang, H., Y. Chen, and D.W. Rosen, *A hybrid geometric modeling method for large scale conformal cellular structures*, in *ASME Computers and Information in Engineering Conference*2006.

18. Wang, H. and D.W. Rosen. *Parametric modeling method for truss structures*. in *ASME Computers and Information in Engineering Conference*. 2002. Montreal.

19. Chen, Y., *An accurate sampling-based method for approximating geometry.* Computer-Aided Design, 2007. **39**(11): p. 975-986.

20. Engelbrecht, S., *Design of meso-scale cellular structure for rapid manufacturing* 2009, Georgia Institute of Technology.

21. Chu, C., Engelbrecht, S., Graf, G.C., Rosen, D.W, *A comparison of synthesis methods for cellular structures with application to additive manufacturing.* Rapid Prototyping Journal, 2010. **16**(4): p. 275-283.

22. Chang, P., *An Improved Size, Matching, and Scaling Synthesis Method for the Design of Meso-Scale Truss Structures*, 2010, Georgia Institute of Techology.

23. Seepersad, C.C., et al., *Robust design of cellular materials with topological and dimension imperfections.* Journal of Mechanical Design, 2006. **128**: p. 1285-1297.

24. Wang, H., *A unit-cell approach for lightweight structure and compliant mechanism*, 2005, Georgia Institute of Technology.

25. Nguyen, J., S.-I. Park, and D.W. Rosen. *Cellular structure design for lightweight components*. in *5th International Conference on Advanced Research and Rapid Prototyping*. 2011. Leiria, Portugal.

26. Malvern, L.E., *Introduction to the Mechanics of a Continuous Medium*. 1969, Upper Saddle River, NJ: Prentice-Hall, Inc.

27. Graf, G., *Development of specialized base primitive for meso-scale conforming truss structures*, 2009, Georgia Institute of Technology.

28. Voorhees, C. *DARPA Asks, " Can You Design, Build, and Fly the Next Generation UAV?"*. 2011 [cited 2012 4/05/2012]; Available from: http://science.dodlive.mil/2011/05/25/darpa-asks-can-you-design-build-and-fly-the-next-generation-uav-video/.

29. Portugal, LF, Judice, JJ, Vicente, LN, A comparison of block pivoting and interior point algorithms for linear least squares problems with nonnegative variables, Mathematics of Computation, 63(1994), pp. 625-643.